Improved high-precision mass measurements of mid-shell neon isotopes

A Jacobs, C Andreoiu, J Bergmann, T Brunner, T Dickel, I Dillmann, E Dunling, J Flowerdew, L Graham, G Gwinner, et al.

Improved high-precision mass measurements of mid-shell neon isotopes

A. Jacobs[a,b], C. Andreoiu[c], J. Bergmann[d,e], T. Brunner[f], T. Dickel[d,e], I. Dillmann[a,g], E. Dunling[a,h], J. Flowerdew[i], L. Graham[a], G. Gwinner[j], Z. Hockenbery[a,f], W.J. Huang[k,l], B. Kootte[a,j], Y. Lan[a,b], K. G. Leach[m], E. Leistenschneider[a,b], D. Lunney[l], E.M. Lykiardopoulou[a,b], V. Monier[h], I. Mukul[a], S.F. Paul[a,n], W.R. Plaß[d,e], M.P. Reiter[a,d,o], C.Scheidenberger[d,e,p], R. Thompson[i], J.L Tracy[a], C. Will[d], M.E. Wieser[i], J. Dilling[a,b], A.A. Kwiatkowski[a,g]

[a] *TRIUMF, Vancouver, V6T 1Z1, British Columbia, Canada*
[b] *Department of Physics and Astronomy, University of British Columbia, Vancouver, V6T 1Z1, British Columbia, Canada*
[c] *Department of Chemistry, Simon Fraser University, Burnaby, V5A 1S6, British Columbia, Canada*
[d] *II. Physikalisches Institut, Justus-Liebig-Universität, Gießen, 35392, Germany*
[e] *GSI Helmholtzzentrum für Schwerionenforschung GmbH, Darmstadt, 64291, Germany*
[f] *Physics Department, McGill University, Montréal, H3A 2T8, Québec, Canada*
[g] *Department of Physics and Astronomy, University of Victoria, Victoria, V8P 5C2, British Columbia, Canada*
[h] *Department of Physics, University of York, York, YO10 5DD, UK*
[i] *Department of Physics and Astronomy, University of Calgary, Calgary, T2N 1N4, Alberta, Canada*
[j] *Department of Physics and Astronomy, University of Manitoba, Winnipeg, R3T 2N2, Manitoba, Canada*
[k] *Advanced Energy Science and Technology Guangdong Laboratory, Huizhou, 516007, China*
[l] *IJCLab-IN2P3-CNRS, Université Paris-Saclay, Orsay, 91405, France*
[m] *Department of Physics, Colorado School of Mines, Golden, 80401, CO, USA*
[n] *Ruprecht-Karls-Universität Heidelberg, Heidelberg, D-69117, Germany*
[o] *Institute for Particle and Nuclear Physics, University of Edinburgh, Edinburgh, EH9 3FD, UK*
[p] *Helmholtz Forschungsakademie Hessen für FAIR (HFHF), Gießen, 35392, Germany*

Abstract

Email address: ajacobs@triumf.ca (A. Jacobs)

New mass values measured with the TITAN MR-TOF-MS are reported for the short-lived isotopes $^{24-26}$Ne, produced at TRIUMF's ISAC facility using a uranium carbide target and cold FEBIAD ion source. A least-squares adjustment using the program which produces the Atomic Mass Evaluation was performed and the improved precision of the new mass values is highlighted. The improved mass accuracy in this $N = 14$ mid-shell region can also point to the refinement in values of the charge radii. By reducing the mass uncertainty of isotopes, their contribution of the mass shift uncertainty in laser spectroscopy can be negated. The work is part of developments for reaching the $N = 20$ Island of Inversion, where high molecular contamination hinders mass measurements of the neon isotopes.

Keywords: mass spectrometry, ion trapping, mass evaluation, nuclear structure

1. Introduction

One key property of all nuclei is their mass. Importantly, the mass of a nucleus is not solely dependent on its constituent parts, protons and neutrons, but also the forces within it. When considered as a whole, these forces amount to a single quantity referred to as the binding energy. Due to the analogous nature of mass and energy, this binding energy causes a shift in the mass of the nucleus such that the final atomic mass is:

$$m(A, Z) = m_p Z + m_n(A - Z) + m_e Z - E_{B_n}/c^2 - E_{B_e}/c^2 \qquad (1)$$

where A is nucleon number, Z is proton number, m_p is proton mass, m_n is neutron mass, m_e is electron mass, E_{B_n} is the nuclear binding energy, and E_{B_e} is electron binding energy.

A prominent description for the organization of these binding forces is the nuclear shell model (1), in which the magic numbers: 2, 8, 20, 28, 50, 82, and 126 arise and are indicative of large energy gaps between nucleon orbitals that increase nuclear stability. However, as experiments push further from stability and reach greater proton-neutron asymmetry, shell effects can diminish and even disappear altogether (2).

One of the most prominent examples of this is the $N = 20$ Island of Inversion, discovered by mass measurements that showed the nuclear binding energy to increase instead of decrease from ^{31}Na to ^{32}Na ($N = 20$ and 21, respectively) (3). Many other experimental observables have also been studied for $N = 20$ and other erstwhile shell closures. For a review see (4).

Since the initial Island of Inversion findings, there have been several high precision mass spectrometry campaigns to map the Island of Inversion borders. Many of those have been pursued using the TITAN spectrometer (5) at TRIUMF's ISAC facility for radioactive ion beams (6; 7; 8). This paper describes our first attempt to address the isotopes of the neon ($Z = 10$) chain. ISAC is a thick-target, ISOL facility from which the radioactive species diffuse as atoms. Since neon is a noble gas, it must be ionized using a discharge source, which unfortunately ionizes many other species in the process. Compounding the problem is the ionization of molecular species formed in the hot environment, causing copious background. In this first attempt, only the isotopes $^{24-26}$Ne could be measured. To go further, a scheme for breaking up the molecules forming the background has been developed, which is the subject of a separate publication (9). Here we present the mass measurement results.

2. The TITAN Experimental Facility

The neon isotopes measured in this experiment were produced at the Isotope Separator and ACcelerator (ISAC) (10) facility located at TRIUMF in Vancouver, Canada. The primary beam of 480 MeV protons with a current of 9.8μA impinged on a UCx target. The neutral product isotopes then diffused out of the target and through a cold transfer line. They were then ionized using a Forced Electron Beam Arc Discharge (FEBIAD) ion source to create the secondary radioactive ion beam (RIB) (11). The combination of ion source and cold transfer line was selected due to the high first ionization potential of Ne as well as the expected presence of large amounts of background species with much lower first ionization potentials (e.g. Na and Mg). Ultimately, the cold transfer line was successful in reducing the rate of Na and Mg relative to Ne by many orders of magnitude.

The RIB is reduced to a single mass unit (i.e. selects for a single A/q) via two dipole mass separators and is then delivered to TRIUMF's Ion Trap for Atomic and Nuclear science (TITAN) (5). The continuous beam from ISAC is accumulated and cooled first in the helium buffer gas filled RFQ cooler and buncher (12) which is set to a potential to match the incoming ≈ 20 keV beam energy. After accumulating for 10 ms, the cold ion bunch is ejected towards the Multi-Reflection Time-of-Flight Mass-Spectrometer (MR-TOF-MS) (13). Between the two traps, the ions pass through a pulsed drift tube which reduces the beam's energy to match that of the MR-TOF-MS's input

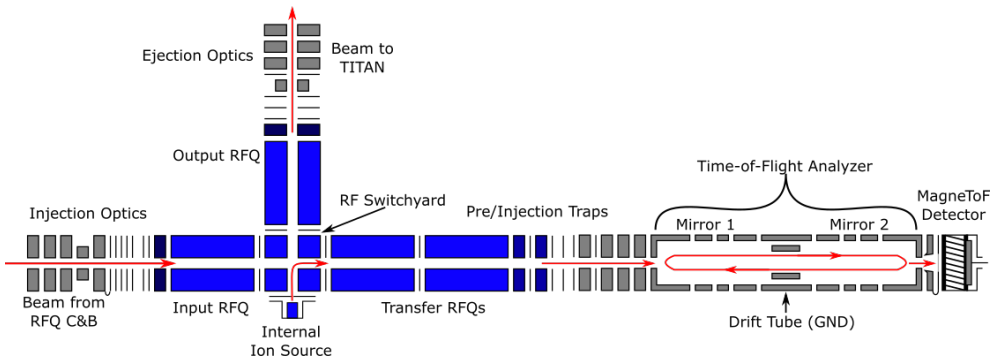

Figure 1: Illustration of the TITAN MR-TOF-MS used to measure the masses in this work. For details, see text.

RFQ ($\approx$ 1.4 keV). The ion bunch is captured in the input RFQ by switching the potential of an entrance aperture from 1.3 kV (transmission) to 1.5 kV (blocking) once the ion bunch is in the RFQ. This allows for additional A/q selection from the TITAN RFQ cooler and buncher to negate any molecular effects due to contamination in the He buffer gas such as charge exchange and molecular adduction. These molecular reactions have been identified with off-line stable molecular beam experiments such as performed in (9).

A schematic of the TITAN MR-TOF-MS is shown in figure 1 (a detailed description is given in (14)). To perform a mass measurement, the captured ions are transported through a six-way RF switchyard (15) and a series of RFQs before undergoing a final cooling stage in the RF injection trap. The ions are then injected into the time-of-flight mass analyzer (16). To confine the ions, the electric potential of the first ion mirror is raised following injection. The ions are then reflected for a set number of turns before the electric potential of the second mirror is lowered and they impinge on a Time-of-Flight (TOF) detector (ETP MagneTOF DM572). The signal from the detector is then converted and recorded using a time-to-digital converter (FastCom TDC MCX6A) to generate a TOF spectrum.

Alternatively, ions can be extracted from the analyzer section by lowering the potential of the first mirror. The ions can then travel back into the injection trap which, when closed at a predetermined time, can recapture a particular species of interest while disposing of the other background species. This process, referred to as mass-selective re-trapping, is a well established technique at the TITAN MR-TOF-MS and enables a background suppression of up to four orders of magnitude with a separation power (the re-trapping

analog to mass resolving power) of 100,000 (17; 18). As a result, a dynamical time focus shift is needed to reach high resolving powers for both the re-trapping and mass measurement cycles, particularly when operated with a different number of turns (19).

Following re-trapping, the ions can be transported back down the MR-TOF-MS RFQs and out to the rest of TITAN or re-injected into the TOF analyzer where a mass measurement will be performed. As such, the TITAN MR-TOF-MS can act as its own isobar separator. An example of a TOF spectrum before and after re-trapping was employed can be seen in top panel of figure 2. Initially, the beam composition is dominated by $^{24}Mg^{+}$ and $^{12}C_2^{+}$. However, with re-trapping, the relative composition of $^{24}Mg^{+}$ and $^{24}Ne^{+}$ shifts by four orders of magnitude while the relative composition of $^{12}C_2^{+}$ and $^{24}Ne^{+}$ shifts by two orders of magnitude. This was done by adjusting the capture time of the trap to ensure there would still be sufficient statistics of $^{12}C_2^{+}$ to perform a calibration. As a result of re-trapping, mass measurements were able to be performed with an isotope of interest to background ratio of $1:10^4$, $1:10^5$, and $1:10^6$ for ^{24}Ne, ^{25}Ne, and ^{26}Ne respectively. The resulting mass spectra can be seen in figure 2 with all species identified.

In this particular experiment, the RFQ cooler and buncher and MR-TOF-MS were operated with a 100 Hz cycle frequency (instead of a more common 30-50 Hz) to accommodate the short half-lives and to reduce the charge-exchange probability in the He buffer-gas-filled RFQs. To accomplish this, two adjustments were needed. First, because a change in switching frequency changes the voltage drop across the HV switches, the analyzer voltages must be re-tuned whenever the cycle frequency is changed. The voltages which define the reflection potential are sensitive to ≈ 10 mV. When the 100 Hz and 50 Hz tunes are compared, a difference in 10 V can be needed to properly readjust the voltages. Second, because the cycle times are shorter than normal, the drag fields of the MR-TOF-MS RFQs needed to be adjusted to ensure all ions travel from the input RFQ to the pre-trap in 2 to 3 ms. As a result of the shorter cycle times, the ion bunches would fly in the TOF analyzer for 380 to 440 turns which corresponds to ≈ 3.7 - 4.4 ms. Due to this shorter flight path, the achieved mass resolving power for this experiment was $\approx 200,000$. Additionally, re-trapping was consistently employed due to the large amount of background. Lastly, the resonant frequency of the RF circuit for the RFQs was boosted from 1.11 MHz to 1.67 MHz to better enable transport of lighter ionic species as described in (14).

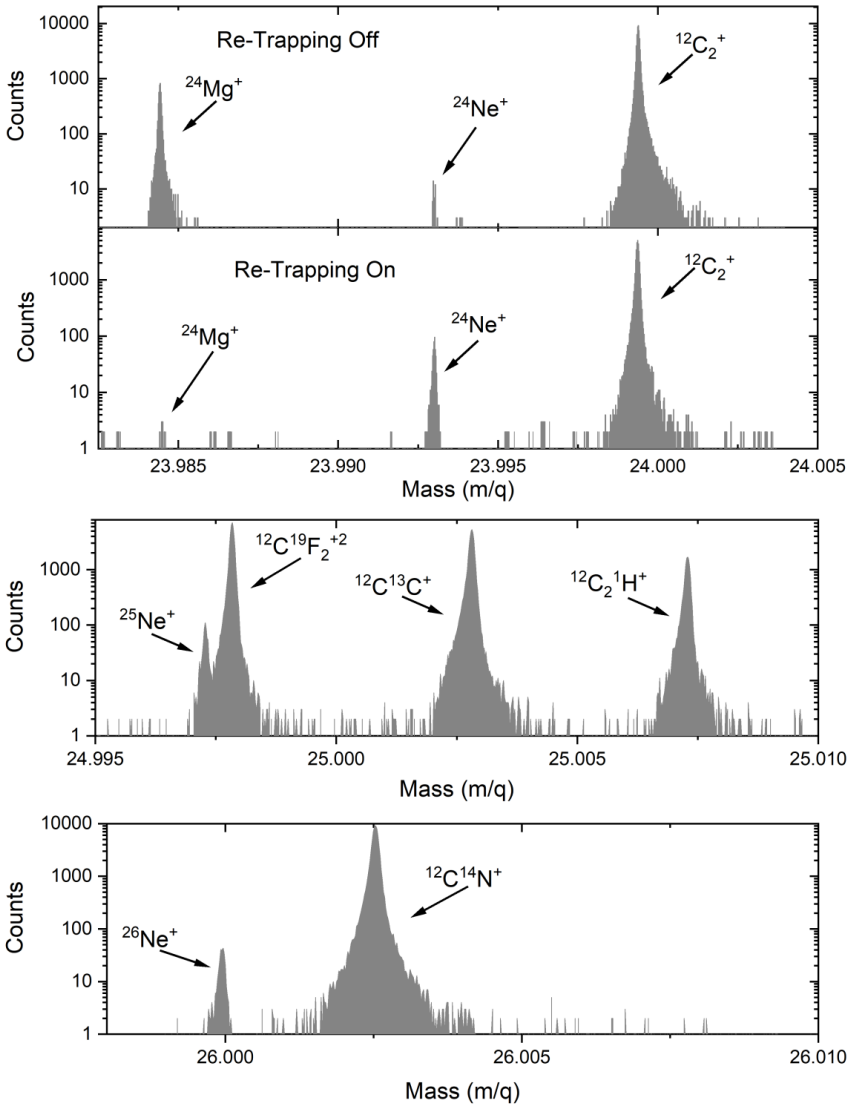

Figure 2: (Top) A comparison of RIB spectra at A/q = 24 with re-trapping on and off. The specific timing for re-trapping in this case was chosen such that the $^{24}Mg^+$ was maximally suppressed while enough $^{12}C_2^+$ remained to perform a mass calibration. The operation of the MR-TOF-MS allowed for a resolving power of $\approx$ 200,000 with $^{24}Ne^+$ and $^{12}C_2^+$ separated by $\approx$ 500 ns in time of flight. (Middle) The RIB spectrum at A/q = 25 with all species identified with re-trapping enabled. (Bottom) The RIB spectrum at A/q = 26 with all species identified with re-trapping enabled.

3. Data Analysis

In general, the data analysis procedure followed the techniques described in (20; 21; 22). Using the home-built Mass Acquisition (MAc) software package (23; 24), the TOF can be converted to mass using:

$$m = c \cdot \frac{(t + t_{\text{start}} - t_0)^2}{(1 + b \cdot T)^2} \tag{2}$$

where c, t_0, and b are calibration parameters, t_{start} is the calculated delay time before triggering the TDC, T is the number of turns done by a species, and t is the measured TOF from the opening of the second mirror. To calibrate the spectrum, t_0 and c are determined using several species spanning multiple mass units before an experiment. In this particular experiment $^{27}Al^+$, $^{28}Si^+$, $^{39}K^+$, and $^{41}K^+$ were used. This allows for b to then be used as the on-line calibration parameter and enables the calibration species to be non-isobaric when accounting for the number of turns, T. In most cases, T for the calibration species and the species of interest is the same, and the formula above can be simplified to: $m = c(t + t_{\text{start}} - t_0)^2$.

After converting a spectrum from TOF to mass, the histogram is exported and fitted using on open-source Python package (25) in which a hyper-exponentially modified Gaussian line shape is used (26). After the centroids of all peaks are determined, a final calibration using

$$\frac{m}{m_{\text{cal}}} = \frac{m_{\text{fit}}}{m_{\text{cal,fit}}} \tag{3}$$

is performed to extract the mass values of each species in the spectrum. This calculation relates the ratio of the fits for the species of interest (m_{fit}) and the calibrant ($m_{\text{cal,fit}}$) to the literature calibrant mass (m_{cal}) and final mass (m) of the species of interest.

As mentioned above, spectra were taken with a different number of turns for each isobar requested from ISAC. Each spectrum underwent an independent fitting analysis, and a weighted mean was taken to obtain a final value. In normal circumstances, a systematic uncertainty is determined using off-line stable-beam tests before and after an experiment. The dominant contribution to the systematic uncertainty was the non-ideal electrical fields during extraction of ions from the analyzer. To test the extent of this effect, the timing for the lowering of the potential of the second electrostatic mirror was scanned and determined the relative systematic uncertainty to be

Species	Calibrant	$\frac{m}{m_{cal}}$	ME_{TITAN} (keV/c^2)	ME_{AME} (keV/c^2)	$ME_{AME2020}$ (keV/c^2)
^{24}Ne	$^{12}C_2$	0.99973367 (31)	-5954.0 (69)	-5951.6 (5)	-5951.6 (5)
^{25}Ne	$^{12}C^{13}C$	0.99977893 (34)	-2023.8 (80)	-2023.5 (78)	-2036 (29)
^{26}Ne	$^{12}C^{14}N$	0.99990063 (33)	456.4 (80)	460.4 (74)	481 (18)

Table 1: Ne mass measurements with their respective calibrants, mass ratios, and mass excess TITAN results (ME_{TITAN}). Additionally, values after AME evaluation with the new TITAN results (ME_{AME}) and AME2020 (29) values are shown. All species were measured in the singly charged (1+) state. Mass Excesses and mass ratios are reported as atomic masses.

$\delta m_{sys}/m = 3 \times 10^{-7}$. This value is in agreement with previously reported systematic uncertainties as seen in (27; 28).

A final precaution is taken for relatively light species measured using the TITAN MR-TOF-MS. Because the ion mirror must be switched open to extract the ions, only a part of a total ion cycle is usable ($\approx$ 60-70%). For light species, the absolute time window for good measurements becomes very small (≈ 9 μs for A/q = 24), and, as a result, the single turn time must be set with a high degree of precision. To determine this window, an off-line scan is done of the opening time of the analyzer to find the region in which the time of flight of the ions is undisturbed (see (20) for a full description of the procedure). To double check this precision, an on-line test measuring the mass of $^{24}Mg^+$ using $^{12}C_2^+$ as a calibrant at a similar number of turns to the subsequent mass measurements while the opening time of the second ion mirror was adjusted confirmed that we correctly set the single turn time. This was confirmed due to the test measurements agreeing with literature values within statistical uncertainty ($\delta m/m \approx 10^{-7}$).

4. Results and Discussion

Table 1 lists the mass values derived for $^{24-26}$Ne, as well as the calibrant ion and corresponding mass ratios. This is reported to accommodate for any eventual changes in calibrant-ion mass. The ratios were input to the Atomic Mass Evaluation, which links all data from mass measurement performed by either mass doublets or by reactions or decays, which can be compared for consistency. This combinatorial evaluation procedure produces the atomic mass table. The new TITAN masses are compared to the literature data in figure 3. Here we describe these different measurements that the AME has linked to provide a final evaluated value.

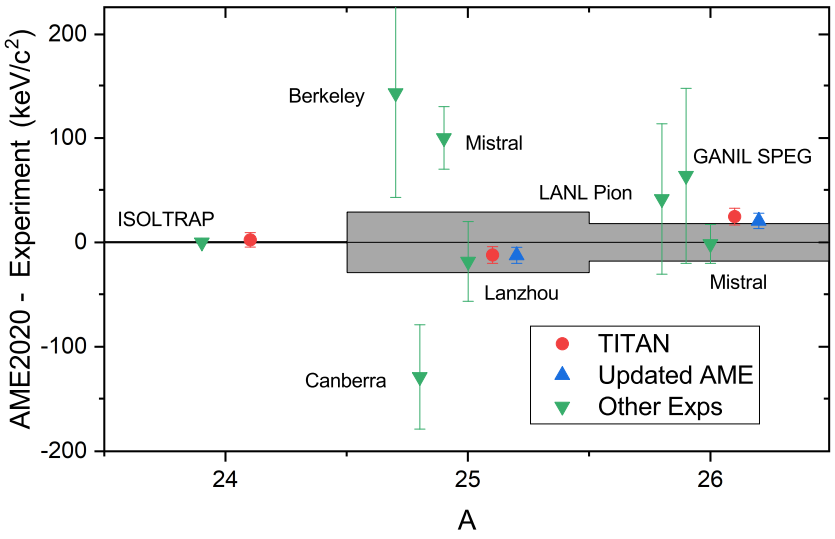

Figure 3: A comparison of the different measurements for ^{24}Ne, ^{25}Ne and ^{26}Ne with the new TITAN results relative to the AME2020. Additionally, the new evaluated masses with the TITAN results are included. The uncertainty in the AME2020 value is shown in gray.

The mass of ^{24}Ne ($T_{1/2}$ = 203 s) was measured by ISOLTRAP (30) using the TOF-ICR method in a Penning trap. The ISOLTRAP value is thirteen times more precise than the new TITAN MR-TOF-MS result but the two values are in excellent agreement. While the new result is given no statistical weight in the AME calculation, the value is still used for a consistency check and slightly strengthens the accuracy for this mass.

The ^{25}Ne ($T_{1/2}$ = 602 ms) mass has been determined via Q values of the reactions ^{26}Mg(^{7}Li,^{8}B)^{25}Ne at Berkeley (31) and ^{26}Mg(^{13}C,^{14}O)^{25}Ne at Canberra (32), by direct mass spectrometry with MISTRAL (33; 34), and by the CSR storage ring at Lanzhou (35). Although the reaction values showed a roughly 2σ deviation, they were averaged in the AME, yielding a mass compatible with our measurement, as is the one from the Lanzhou storage ring. The MISTRAL value deviated by 3.4σ from the evaluated mass so was rejected from the AME since the mass spectrum showed a double peak. Coincidentally, the TITAN MR-TOF-MS was able to resolve a near lying double peak caused by ^{12}C^{19}F$_2^{2+}$ which could have been the cause of the previously reported double peak. The TITAN MR-TOF-MS reached a resolving power of $\approx$ 200,000 in this experiment what the required resolving

power to separate these two species is ≈ 40,000. The TITAN result now accounts for 93% of the AME value.

The mass of ^{26}Ne ($T_{1/2} = 197$ ms) has been determined via Q value of the pion-exchange reaction ^{26}Mg(π^-,π^+)^{26}Ne at Los Alamos (36) and directly by magnetic rigidity combined with time of flight using SPEG at GANIL (37) and the RF spectrometer MISTRAL (33; 34). All of the data are in agreement but the superior precision of the new TITAN value accounts 83% of the new evaluated mass.

Nuclear structure effects can be nicely revealed using both the two-neutron separation energy (S_{2n}):

$$S_{2N}(N,Z) = [m(N-2,Z) - m(N,Z) + 2m_n] \cdot c^2 \tag{4}$$

and the empirical shell gap (ΔS_{2N}):

$$\Delta S_{2N}(N,Z) = S_{2N}(N,Z) - S_{2N}(N+2,Z) \tag{5}$$

The S_{2n} and ΔS_{2N} values for the neon isotopes calculated from the AME (29) and the new values are plotted in figure 4. While the values have changed very little with the new, improved, masses, they are now more accurate due to the good agreement with previous data. Additionally, the S_{2n} and ΔS_{2N} from different mass models are compared to the experimental data. In general, the models accurately recreate the trends seen in both the S_{2n} and ΔS_{2N}, particularly, a local minimum in ΔS_{2N} at N = 12 or 13 and local maximum at N = 15.

Figure 5 superimposes both the empirical shell gap as well as the difference in mean-square charge radii, obtained from laser spectroscopy (41) along the neon isotopic chain. The ΔS_{2n} values reflect the gain in binding energy from the $d_{5/2}$ sub-shell closure at $N = 15$ whereas the charge radius is lowest for $N = 14$, raising the question of a new magic number, in place of $N = 20$. This point is discussed by Marinova et al. (41), who also included the results of microscopic Fermionic Molecular Dynamics (FMD) calculations that include contributions from clustering from work on the lighter neon isotopes (42). As mentioned in both laser spectroscopy papers (41; 42), a source of systematic uncertainty in the charge radii is from the mass shift as depicted in figure 5. However, for high precision mass measurements, the contribution to the final uncertainty is ≈ 0.01% (42). Thus, the new mass data will also reduce the uncertainties of these observables to better refine the transition

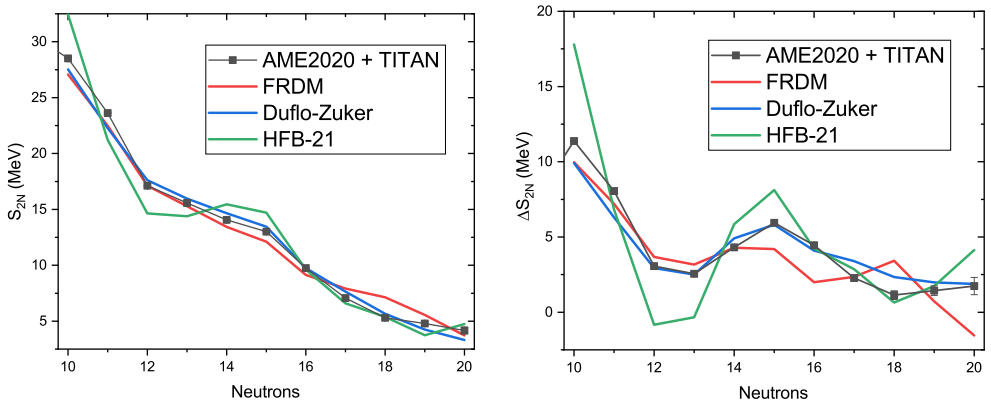

Figure 4: The two-neutron separation energy (S_{2n}, Left) and empirical shell gap (ΔS_{2N}, Right) for the chain of ($Z = 10$) neon isotopes (calculated using the new masses combined with those from the AME2020 (29)). The new experimental data is combined with mean-field calculations using FRDM (38), Duflo-Zuker (39), and HFB-21 (40).

towards the $N = 20$ Island of Inversion, and serves as a motivating factor to perform high precision mass measurements beyond ^{26}Ne.

5. Conclusion

New mass values for the short-lived $^{24-26}$Ne isotopes are reported and a mass evaluation was performed. The value for ^{24}Ne is in good agreement with a more precise Penning-trap value (30) while the precisions for the heavier two were improved by factors of more than three and two, respectively. The new precision mass values can eventually help reduce the uncertainties of the charge radii for these isotopes (41). It would the interesting to extend the FMD calculations from the lighter neon isotopes (42) to see if cluster configurations continue to account for some of the binding energy. Since the experimental campaign described in this work, several technical initiatives have been undertaken to extend the reach of the TITAN MR-TOF-MS into the $N = 20$ Island of Inversion with Ne including the development of collision-induced dissociation (43; 9) and improvements to He buffer gas quality.

Acknowledgements

This work was partially supported by Canadian agencies NSERC and CFI, U.S.A. DOE (grant DE-FG02-93ER40789), Brazil's CNPq (grant no.

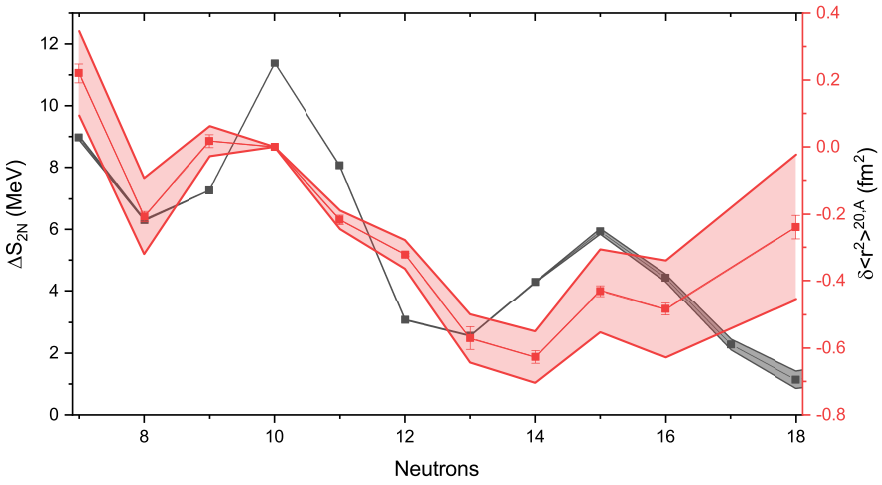

Figure 5: The empirical shell gap (ΔS_{2n}) for the chain of ($Z = 10$) neon isotopes (calculated using the new masses combined with those from the AME2020 (29)), superimposed with the mean-square charge radii from (41). The statistical uncertainty is shown via red error bars while they systematic uncertainty, resulting largely from unknown mass shifts, is shown by the lightly shaded red area.

249121/2013-1), the Canada-UK Foundation, France's *Programme International de Coopération Scientifique* PACIFIC, German institutions DFG (grants FR 601/3-1, SCHE 1969/2-1 and SFB 1245 and through PRISMA Cluster of Excellence), BMBF (grants 05P19RGFN1 and 05P21RGFN1), and by the JLU and GSI under the JLU-GSI strategic Helmholtz partnership agreement.

References

[1] M. Goeppert Mayer, J. H. Jensen, Elementary Theory of Nuclear Shell Structure, John Wiley and Sons, New York, 1955.

[2] D. Warner, Not-so-magic numbers, Nature 430 (2004) 517–519. doi:10.1038/430517a.

[3] C. Thibault, R. Klapisch, C. Rigaud, A. M. Poskanzer, R. Prieels, L. Lessard, W. Reisdorf, Direct measurement of the masses of ^{11}Li and $^{26-32}$Na with an on-line mass spectrometer, Phys. Rev. C 12 (2) (1975) 644–657. doi:10.1103/PhysRevC.12.644.

[4] O. Sorlin, M.-G. Porquet, Nuclear magic numbers: New features far from stability, Progress in Particle and Nuclear Physics 61 (2) (2008) 602–673. doi:https://doi.org/10.1016/j.ppnp.2008.05.001.
URL https://www.sciencedirect.com/science/article/pii/S0146641008000380

[5] J. Dilling, P. Bricault, M. Smith, H. J. Kluge, The proposed TITAN facility at ISAC for very precise mass measurements on highly charged short-lived isotopes, Nucl. Instrum. Meth. Phys. Res. B 204 (2003) 492–496. doi:10.1016/S0168-583X(02)02118-3.

[6] A. Chaudhuri, C. Andreoiu, T. Brunner, U. Chowdhury, S. Ettenauer, A. T. Gallant, G. Gwinner, A. A. Kwiatkowski, A. Lennarz, D. Lunney, T. D. Macdonald, B. E. Schultz, M. C. Simon, V. V. Simon, J. Dilling, Evidence for the extinction of the N=20 neutron-shell closure for 32Mg from direct mass measurements, Phys. Rev. C 88 (5) (2013) 054317. doi:10.1103/PhysRevC.88.054317.

[7] A. A. Kwiatkowski, C. Andreoiu, J. C. Bale, A. Chaudhuri, U. Chowdhury, S. Malbrunot-Ettenauer, A. T. Gallant, A. Grossheim, G. Gwinner, A. Lennarz, T. D. Macdonald, T. J. Rauch, B. E. Schultz, S. Seeraji, M. C. Simon, V. V. Simon, D. Lunney, A. Poves, J. Dilling, Observation of a crossover of S2n in the island of inversion from precision mass spectrometry, Phys. Rev. C 92 (6) (2015) 061301. doi:10.1103/PhysRevC.92.061301.

[8] A. T. Gallant, M. Alanssari, J. C. Bale, C. Andreoiu, B. R. Barquest, U. Chowdhury, J. Even, A. Finlay, D. Frekers, G. Gwinner, R. Klawitter, B. Kootte, A. A. Kwiatkowski, D. Lascar, K. G. Leach, E. Leistenschneider, A. Lennarz, A. J. Mayer, D. Short, R. Thompson, M. Wieser, D. Lunney, J. Dilling, Mass determination near N=20 for Al and Na isotopes, Physical Review C 96 (2) (2017) 1–5. doi:10.1103/PhysRevC.96.024325.

[9] A. Jacobs, C. Andreoiu, J. Bergmann, T. Brunner, T. Dickel, I. Dillmann, E. Dunling, J. Flowerdew, L. Graham, G. Gwinner, Z. Hockenbery, B. Kootte, Y. Lan, K. Leach, E. Leistenschneider, E. Lykiardopoulou, V. Monier, I. Mukul, S. Paul, W. Plaß, M. Reiter, C. Scheidenberger, R. Thompson, J. Tracy, C. Will, M. Wieser, M. Yavor, J. Dilling, A. Kwiatkowski, Collision-induced dissociation at triumf's ion

trap for atomic and nuclear science, International Journal of Mass Spectrometry (2022) 116931doi:https://doi.org/10.1016/j.ijms.2022.116931.
URL https://www.sciencedirect.com/science/article/pii/S1387380622001361

[10] G. C. Ball, L. Buchmann, B. Davids, R. Kanungo, C. Ruiz, C. E. Svensson, Physics with reaccelerated radioactive beams at TRIUMF-ISAC, Journal of Physics G: Nuclear and Particle Physics 38 (2) (2011). doi:10.1088/0954-3899/38/2/024003.

[11] B. E. Schultz, J. Sandor, P. Kunz, A. Mjøs, O. Kester, F. Ames, FEBIAD Ion Source Development At TRIUMF-ISAC, in: 9th International Particle Accelerator Conference (IPAC '18), Vancouver, Canada, 2018, p. THPML041. doi:10.18429/JACoW-IPAC2018-THPML041.

[12] T. Brunner, M. J. Smith, M. Brodeur, S. Ettenauer, A. T. Gallant, V. V. Simon, A. Chaudhuri, A. Lapierre, E. Mané, R. Ringle, M. C. Simon, J. A. Vaz, P. Delheij, M. Good, M. R. Pearson, J. Dilling, TITAN's digital RFQ ion beam cooler and buncher, operation and performance, Nucl. Instrum. Meth. Phys. Res. A 676 (2012) 32–43. doi:10.1016/j.nima.2012.02.004.

[13] C. Jesch, T. Dickel, W. R. Plaß, D. Short, S. A. San Andres, J. Dilling, H. Geissel, F. Greiner, J. Lang, K. G. Leach, W. Lippert, C. Scheidenberger, M. I. Yavor, The MR-TOF-MS isobar separator for the TITAN facility at TRIUMF, Hyperfine Interact 235 (2015) 97–106. doi:10.1007/s10751-015-1184-2.

[14] M. Reiter, S. A. S. Andrés, J. Bergmann, T. Dickel, J. Dilling, A. Jacobs, A. Kwiatkowski, W. Plaß, C. Scheidenberger, D. Short, C. Will, C. Babcock, E. Dunling, A. Finlay, C. Hornung, C. Jesch, R. Klawitter, B. Kootte, D. Lascar, E. Leistenschneider, T. Murböck, S. Paul, M. Yavor, Commissioning and performance of titan's multiple-reflection time-of-flight mass-spectrometer and isobar separator, Nuclear Instruments and Methods in Physics Research Section A: Accelerators, Spectrometers, Detectors and Associated Equipment 1018 (2021) 165823. doi:https://doi.org/10.1016/j.nima.2021.165823.
URL https://www.sciencedirect.com/science/article/pii/S0168900221008081

[15] W. R. Plaß, T. Dickel, S. San Andres, J. Ebert, F. Greiner, C. Hornung, C. Jesch, J. Lang, W. Lippert, T. Majoros, D. Short, H. Geissel, E. Haet-

tner, M. P. Reiter, A. K. Rink, C. Scheidenberger, M. I. Yavor, High-performance multiple-reflection time-of-flight mass spectrometers for research with exotic nuclei and for analytical mass spectrometry, Physica Scripta 2015 (T166) (2015). doi:10.1088/0031-8949/2015/T166/014069.

[16] M. I. Yavor, W. R. Plaß, T. Dickel, H. Geissel, C. Scheidenberger, Ion-optical design of a high-performance multiple-reflection time-of-flight mass spectrometer and isobar separator, International Journal of Mass Spectrometry (2015). doi:10.1016/j.ijms.2015.01.002.

[17] T. Dickel, W. R. Plaß, W. Lippert, J. Lang, M. I. Yavor, H. Geissel, C. Scheidenberger, Isobar Separation in a Multiple-Reflection Time-of-Flight Mass Spectrometer by Mass-Selective Re-Trapping, Journal of The American Society for Mass Spectrometry (2017). doi:10.1007/s13361-017-1617-z.

[18] S. Beck, B. Kootte, I. Dedes, T. Dickel, A. A. Kwiatkowski, E. M. Lykiardopoulou, W. R. Plaß, M. P. Reiter, C. Andreoiu, J. Bergmann, T. Brunner, D. Curien, J. Dilling, J. Dudek, E. Dunling, J. Flowerdew, A. Gaamouci, L. Graham, G. Gwinner, A. Jacobs, R. Klawitter, Y. Lan, E. Leistenschneider, N. Minkov, V. Monier, I. Mukul, S. F. Paul, C. Scheidenberger, R. I. Thompson, J. L. Tracy, M. Vansteenkiste, H.-L. Wang, M. E. Wieser, C. Will, J. Yang, Mass measurements of neutron-deficient yb isotopes and nuclear structure at the extreme proton-rich side of the $n = 82$ shell, Phys. Rev. Lett. 127 (2021) 112501. doi:10.1103/PhysRevLett.127.112501.
URL `https://link.aps.org/doi/10.1103/PhysRevLett.127.112501`

[19] T. Dickel, M. I. Yavor, J. Lang, W. R. Plaß, W. Lippert, H. Geissel, C. Scheidenberger, Dynamical time focus shift in multiple-reflection time-of-flight mass spectrometers, International Journal of Mass Spectrometry 412 (2017). doi:10.1016/j.ijms.2016.11.005.

[20] S. Ayet San Andrés, C. Hornung, J. Ebert, W. R. Plaß, T. Dickel, H. Geissel, C. Scheidenberger, J. Bergmann, F. Greiner, E. Haettner, C. Jesch, W. Lippert, I. Mardor, I. Miskun, Z. Patyk, S. Pietri, A. Pihktelev, S. Purushothaman, M. P. Reiter, A. K. Rink, H. Weick, M. I. Yavor, S. Bagchi, V. Charviakova, P. Constantin, M. Diwisch, A. Finlay, S. Kaur, R. Knöbel, J. Lang, B. Mei, I. D. Moore, J. H. Otto,

I. Pohjalainen, A. Prochazka, C. Rappold, M. Takechi, Y. K. Tanaka, J. S. Winfield, X. Xu, High-resolution, accurate multiple-reflection time-of-flight mass spectrometry for short-lived, exotic nuclei of a few events in their ground and low-lying isomeric states, Physical Review C 99 (064313) (2019). doi:10.1103/PhysRevC.99.064313.

[21] S. F. Paul, J. Bergmann, J. D. Cardona, K. A. Dietrich, E. Dunling, Z. Hockenbery, C. Hornung, C. Izzo, A. Jacobs, A. Javaji, B. Kootte, Y. Lan, E. Leistenschneider, E. M. Lykiardopoulou, I. Mukul, T. Murböck, W. S. Porter, R. Silwal, M. B. Smith, J. Ringuette, T. Brunner, T. Dickel, I. Dillmann, G. Gwinner, M. MacCormick, M. P. Reiter, H. Schatz, N. A. Smirnova, J. Dilling, A. A. Kwiatkowski, Mass measurements of $^{60-63}$Ga reduce x-ray burst model uncertainties and extend the evaluated $t = 1$ isobaric multiplet mass equation, Phys. Rev. C 104 (2021) 065803. doi:10.1103/PhysRevC.104.065803.
URL https://link.aps.org/doi/10.1103/PhysRevC.104.065803

[22] E. Dunling, in preparation.

[23] T. Dickel, S. A. San Andrés, S. Beck, J. Bergmann, J. Dilling, F. Greiner, C. Hornung, A. Jacobs, G. Kripko-Koncz, A. Kwiatkowski, E. Leistenschneider, A. Pikthtelev, W. R. Plaß, M. P. Reiter, C. Scheidenberger, C. Will, Recent upgrades of the multiple-reflection time-of-flight mass spectrometer at TITAN, TRIUMF, Hyperfine Interactions 240 (1) (2019). doi:10.1007/s10751-019-1610-y.

[24] J. Bregmann, In preparation, Ph.D. thesis, JLU-Giessen.

[25] S. F. Paul, emgfit - Fitting of time-of-flight mass spectra with hyper-EMG models (Dec. 2020). doi:10.5281/zenodo.4731019.
URL https://doi.org/10.5281/zenodo.4731019

[26] S. Purushothaman, S. Ayet San Andrés, J. Bergmann, T. Dickel, J. Ebert, H. Geissel, C. Hornung, W. Plaß, C. Rappold, C. Scheidenberger, Y. Tanaka, M. Yavor, Hyper-emg: A new probability distribution function composed of exponentially modified gaussian distributions to analyze asymmetric peak shapes in high-resolution time-of-flight mass spectrometry, International Journal of Mass Spectrometry 421 (2017) 245–254. doi:https://doi.org/10.1016/j.ijms.2017.07.014.
URL https://www.sciencedirect.com/science/article/pii/S1387380616302913

[27] E. Leistenschneider, M. P. Reiter, S. A. San Andrés, B. Kootte, J. D. Holt, P. Navrátil, C. Babcock, C. Barbieri, B. R. Barquest, J. Bergmann, J. Bollig, T. Brunner, E. Dunling, A. Finlay, H. Geissel, L. Graham, F. Greiner, H. Hergert, C. Hornung, C. Jesch, R. Klawitter, Y. Lan, D. Lascar, K. G. Leach, W. Lippert, J. E. McKay, S. F. Paul, A. Schwenk, D. Short, J. Simonis, V. Somà, R. Steinbrügge, S. R. Stroberg, R. Thompson, M. E. Wieser, C. Will, M. I. Yavor, C. Andreoiu, T. Dickel, I. Dillmann, G. Gwinner, W. R. Plaß, C. Scheidenberger, A. A. Kwiatkowski, J. Dilling, Dawning of the N = 32 Shell Closure Seen through Precision Mass Measurements of Neutron-Rich Titanium Isotopes, Phys. Rev. Lett. 120 (6) (2018) 62503. doi:10.1103/PhysRevLett.120.062503.

[28] M. P. Reiter, S. A. San Andrés, E. Dunling, B. Kootte, E. Leistenschneider, C. Andreoiu, C. Babcock, B. R. Barquest, J. Bollig, T. Brunner, I. Dillmann, A. Finlay, G. Gwinner, L. Graham, J. D. Holt, C. Hornung, C. Jesch, R. Klawitter, Y. Lan, D. Lascar, J. E. McKay, S. F. Paul, R. Steinbrügge, R. Thompson, J. L. Tracy, M. E. Wieser, C. Will, T. Dickel, W. R. Plaß, C. Scheidenberger, A. A. Kwiatkowski, J. Dilling, Quenching of the N=32 neutron shell closure studied via precision mass measurements of neutron-rich vanadium isotopes, Phys. Rev. C 98 (2) (2018) 024310. doi:10.1103/PhysRevC.98.024310.

[29] M. Wang, W. J. Huang, F. G. Kondev, G. Audi, S. Naimi, The AME 2020 atomic mass evaluation (II). Tables, graphs and references, Chinese Physics C 45 (3) (2021). doi:10.1088/1674-1137/abddaf.

[30] K. Blaum, G. Audi, D. Beck, G. Bollen, C. Guénaut, P. Delahaye, F. Herfurth, A. Kellerbauer, H.-J. Kluge, D. Lunney, D. Rodríguez, S. Schwarz, L. Schweikhard, C. Weber, C. Yazidjian, Recent results from the penning trap mass spectrometer isoltrap, Nuclear Physics A 746 (2004) 305–310, proceedings of the Sixth International Conference on Radioactive Nuclear Beams (RNB6). doi:https://doi.org/10.1016/j.nuclphysa.2004.09.028.
URL https://www.sciencedirect.com/science/article/pii/S0375947404009911

[31] K. H. Wilcox, N. A. Jelley, G. J. Wozniak, R. B. Weisenmiller, H. L. Harney, J. Cerny, New spectroscopic measurements via exotic nuclear rearrangement: The reaction ^{26}Mg(^{7}Li, ^{8}B) ^{25}Ne, Phys. Rev. Lett. 30

(1973) 866–869. doi:10.1103/PhysRevLett.30.866.
URL https://link.aps.org/doi/10.1103/PhysRevLett.30.866

[32] C. Woods, L. Fifield, R. Bark, P. Drumm, M. Hotchkis, A study of ^{25}Ne via the ^{26}Mg(^{13}C,^{14}O)^{25}Ne reaction, Nuclear Physics A 437 (2) (1985) 454–464. doi:https://doi.org/10.1016/S0375-9474(85)90101-0.
URL https://www.sciencedirect.com/science/article/pii/S0375947485901010

[33] D. Lunney, C. Monsanglant, G. Audi, G. Bollen, C. Borcea, H. Doubre, C. Gaulard, S. Henry, M. deSaintSimon, C. Thibault, C. Toader, N. Vieira, Recent results on ne and mg from the mistral mass measurement program at isolde, Hyperfine Interactions 132 (1) (2001) 297–305. doi:10.1023/A:1011952114837.
URL https://doi.org/10.1023/A:1011952114837

[34] C. Gaulard, G. Audi, C. Bachelet, D. Lunney, M. de Saint Simon, C. Thibault, N. Vieira, Accurate mass measurements of ^{26}Ne,$^{26–30}$Na,$^{29–33}$Mg performed with the mistral spectrometer, Nuclear Physics A 766 (2006) 52–73. doi:https://doi.org/10.1016/j.nuclphysa.2005.12.007.
URL https://www.sciencedirect.com/science/article/pii/S0375947405012431

[35] X. Xu, M. Wang, Y.-H. Zhang, H.-S. Xu, P. Shuai, X.-L. Tu, Y. A. Litvinov, X.-H. Zhou, B.-H. Sun, Y.-J. Yuan, J.-W. Xia, J.-C. Yang, K. Blaum, R.-J. Chen, X.-C. Chen, C.-Y. Fu, Z. Ge, Z.-G. Hu, W.-J. Huang, D.-W. Liu, Y.-H. Lam, X.-W. Ma, R.-S. Mao, T. Uesaka, G.-Q. Xiao, Y.-M. Xing, T. Yamaguchi, Y. Yamaguchi, Q. Zeng, X.-L. Yan, H.-W. Zhao, T.-C. Zhao, W. Zhang, W.-L. Zhan, Direct mass measurements of neutron-rich ^{86}Kr projectile fragments and the persistence of neutron magic number n=32 in sc isotopes*, Chinese Physics C 39 (10) (2015) 104001. doi:10.1088/1674-1137/39/10/104001.
URL https://dx.doi.org/10.1088/1674-1137/39/10/104001

[36] H. Nann, K. K. Seth, S. Iversen, M. Kaletka, D. Barlow, D. Smith, Identification and measurement of the mass of ^{26}Ne(g.s.) by the ^{26}Mg$(\pi,\pi+)^{26}$Ne reaction, Physics Letters B 96 (3) (1980) 261–264. doi:https://doi.org/10.1016/0370-2693(80)90762-5.
URL https://www.sciencedirect.com/science/article/pii/0370269380907625

[37] N. Orr, W. Mittig, L. Fifield, M. Lewitowicz, E. Plagnol, Y. Schutz, Z. Wen Long, L. Bianchi, A. Gillibert, A. Belozyorov, S. Lukyanov, Y. Penionzhkevich, A. Villari, A. Cunsolo, A. Foti, G. Audi, C. Stephan, L. Tassan-Got, New mass measurements of neutron-rich nuclei near n=20, Physics Letters B 258 (1) (1991) 29–34. doi:https://doi.org/10.1016/0370-2693(91)91203-8.
URL https://www.sciencedirect.com/science/article/pii/0370269391912038

[38] P. Möller, A. Sierk, T. Ichikawa, H. Sagawa, Nuclear ground-state masses and deformations: Frdm(2012), Atomic Data and Nuclear Data Tables 109-110 (2016) 1–204. doi:https://doi.org/10.1016/j.adt.2015.10.002.
URL https://www.sciencedirect.com/science/article/pii/S0092640X1600005X

[39] J. Duflo, A. Zuker, Microscopic mass formulas, Phys. Rev. C 52 (1995) R23–R27. doi:10.1103/PhysRevC.52.R23.
URL https://link.aps.org/doi/10.1103/PhysRevC.52.R23

[40] S. Goriely, N. Chamel, J. M. Pearson, Further explorations of skyrme-hartree-fock-bogoliubov mass formulas. xii. stiffness and stability of neutron-star matter, Phys. Rev. C 82 (2010) 035804. doi:10.1103/PhysRevC.82.035804.
URL https://link.aps.org/doi/10.1103/PhysRevC.82.035804

[41] K. Marinova, W. Geithner, M. Kowalska, K. Blaum, S. Kappertz, M. Keim, S. Kloos, G. Kotrotsios, P. Lievens, R. Neugart, H. Simon, S. Wilbert, Charge radii of neon isotopes across the *sd* neutron shell, Phys. Rev. C 84 (2011) 034313. doi:10.1103/PhysRevC.84.034313.
URL https://link.aps.org/doi/10.1103/PhysRevC.84.034313

[42] W. Geithner, T. Neff, G. Audi, K. Blaum, P. Delahaye, H. Feldmeier, S. George, C. Guénaut, F. Herfurth, A. Herlert, S. Kappertz, M. Keim, A. Kellerbauer, H.-J. Kluge, M. Kowalska, P. Lievens, D. Lunney, K. Marinova, R. Neugart, L. Schweikhard, S. Wilbert, C. Yazidjian, Masses and charge radii of $^{17-22}$Ne and the two-proton-halo candidate ^{17}Ne, Phys. Rev. Lett. 101 (2008) 252502. doi:10.1103/PhysRevLett.101.252502.
URL https://link.aps.org/doi/10.1103/PhysRevLett.101.252502

[43] A. Jacobs, Collision Induced Dissociation and Mass Spectrometry with the TITAN Multiple-Reflection Time-of-Flight Mass Spectrometer, Master's thesis, University of British Columbia (2019).